Surface Modification

DOI: 10.1002/anie.201406911

Polymer-Induced Surface Modifications of Pd-based Thin Films Leading to Improved Kinetics in Hydrogen Sensing and Energy Storage Applications**

Peter Ngene, Ruud J. Westerwaal, Sumit Sachdeva, Wim Haije, Louis C. P. M. de Smet, and Bernard Dam*

Abstract: *The catalytic properties of Pd alloy thin films are enhanced by a thin sputtered PTFE coating, resulting in profound improvements in hydrogen adsorption and desorption in Pd-based and Pd-catalyzed hydrogen sensors and hydrogen storage materials. The remarkably enhanced catalytic performance is attributed to chemical modifications of the catalyst surface by the sputtered PTFE leading to a possible change in the binding strength of the intermediate species involved in the hydrogen sorption process.*

Due to the high and selective affinity of palladium toward hydrogen, Pd-based thin films are used in a variety of (de)hydrogenation processes.[1,2] These include H_2 sensors,[3,4] membranes for H_2 separation,[5] membranes for direct production of H_2O_2 from H_2 and O_2,[6] and as efficient catalysts in smart windows, H_2 sensing, and H_2 storage applications.[7–11] When molecular H_2 reaches the Pd (or Pd-alloy) surface, it dissociates rapidly into atomic hydrogen (H). The atomic hydrogen can react with other reactants on the Pd surface to form product molecules or may diffuse into the bulk of Pd. The latter case is associated with a reversible change in the optical, structural, and electronic properties of Pd, which can be exploited to detect the presence of H_2.[1,3,4,12–14] It has been shown that the catalytic and sensing properties of metals such as Pd are generally related to the electronic structure of the surface atoms in particular,[15–17] which determines the nature and extent to which reactants interact with (bind to) the metal surface.[15,17–19] A change in the electronic structure of the surface may therefore lead to a significant change in the performance. Thus significant efforts have been made to tailor the catalytic performance of metals by modification of the surface electronic properties.[18,20–22] Electronic modification of Pd nanoparticles has been successfully achieved by alloying,[23,24] creating core–shell structures,[25,26] and by tuning the metal–support interaction.[27,28]

Here, we show that a thin sputter-deposited polymer coating significantly alters the catalytic properties of Pd and Pd–Au alloy thin films. Sputtered polytetrafluoroethylene (PTFE) has earlier been used in Pd-based H_2 sensors as a hydrophobic material to protect Pd from water-based contaminants.[11,29,30] We show for the first time that it actually leads to a significant modification of the catalytic properties of the Pd and Pd–Au surface. It appears that Pd−CF_x bonds are formed at the surface, resulting in a change in the electron binding energy of the surface Pd atoms. Therefore we attribute the remarkable increase in the hydrogen absorption and desorption kinetics to a change in the binding strength of the intermediate species involved in the (de)hydrogenation reactions, resulting from a modification of the catalyst surface by the sputter-deposited PTFE layer.

In Figure 1 the effect of PTFE on the performance of a Pd-catalyzed H_2 detector is shown. In this case, Pd only serves as a selective filter for hydrogen, whereas yttrium (Y) is the actual sensing layer. The large optical changes occurring in Y on the formation of the dihydride and trihydride phases are visible by the naked eye.[10] Figure 1 A shows the configuration of this eye-readable H_2 detector (See the Supporting Information (SI) for experimental details). On top of the 60 nm Y layer is a 50 nm Pd_xAu_{1-x} thin film catalyst, which is also capped with a 15 nm layer of sputtered PTFE. In the presence of H_2, the Pd_xAu_{1-x} thin film enables the dissociation of molecular H_2 into atomic hydrogen, which diffuses rapidly through the Pd_xAu_{1-x} layer, leading to hydrogenation of Y to $YH_{1.9}$, $YH_{2.1}$, and YH_3, depending on the H_2 pressure. The different optical properties of the three YH_x states allow for the detection of H_2 at < 5 ppm ($YH_{1.9}$), ≥ 5 ppm ($YH_{2.1}$), and 0.01 vol% or 100 ppm (YH_3).[10] Upon exposure of the hydrogenated samples to air or O_2 at room temperature, the Pd_xAu_{1-x} catalyzes the dehydrogenation of YH_3 to $YH_{1.9}$, accompanied by the formation of H_2O on the surface.[31–33] It is important to note that although Pd_xAu_{1-x} also undergoes a small reversible optical change, in this configuration it is not

[*] Dr. P. Ngene, Dr. R. J. Westerwaal, Dr. W. Haije, Prof. Dr. B. Dam
Materials for Energy Conversion and Storage (MECS)
Department of Chemical Engineering
Delft University of Technology
Delft (The Netherlands)
E-mail: p.ngene@tudelft.nl
S. Sachdeva, Dr. L. C. P. M. de Smet
Organic Materials & Interface (OMI)
Department of Chemical Engineering
Delft University of Technology
Delft (The Netherlands)
Dr. W. Haije
Energy Research Centre of the Netherlands (ECN)
P.O Box 1, 1755 ZG Petten (The Netherlands)

[**] We acknowledge financial support from the Netherlands Organisation for Scientific Research (NWO, ACTS Sustainable Hydrogen Program), the NanoNextNL of the Government of the Netherlands, and 130 partners. Hermans Schreuders is acknowledged for technical support.

Supporting information for this article is available on the WWW under http://dx.doi.org/10.1002/anie.201406911.

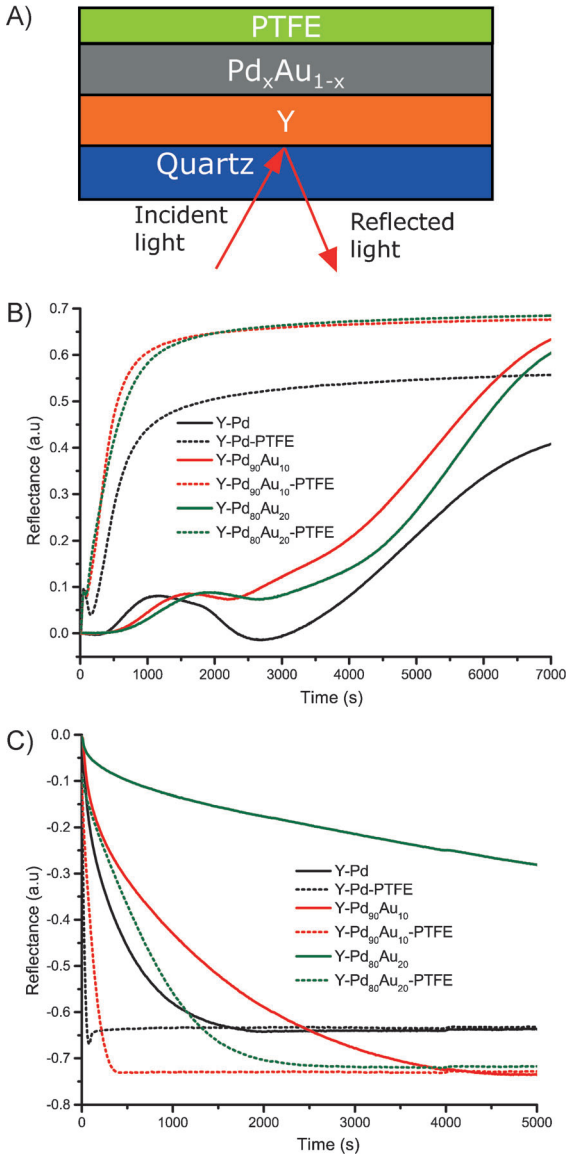

Figure 1. Effect of sputtered PTFE on the kinetic properties of Pd- and Pd–Au-coated Y thin film sensing layers. A) Configuration of the H_2 detector. B) Response of the detectors to 0.105 mbar H_2 at room temperature. C) Dehydrogenation of the loaded detector in a 20 mL min^{-1} flow of 20% O_2/Ar.

the active sensing material but it mainly serves as a selective catalyst for hydrogenation (loading) and dehydrogenation (unloading) of the Y-sensing layer.[10]

Figure 1 B compares the change in reflectance of detectors with different catalyst layer (with or without PTFE), on exposure to 0.105 mbar H_2 at room temperature. The samples without PTFE did not show the full optical transition even after exposure for 7000 s (1 h, 56 min) meaning that these samples are not fully hydrogenated from $YH_{1.9} \rightarrow YH_3$. Since the equilibrium pressure for the formation of YH_3 is 0.1 mbar H_2 at room temperature, very rapid hydrogenation of the samples is unexpected at 0.105 mbar H_2 due to kinetic limitations resulting from the low chemical potential. Remarkably, full hydrogenation to YH_3 occurred in the samples with PTFE top layer, in less than 1000 s. The samples containing Pd–Au alloy catalysts show slightly faster kinetics than the pure Pd. Clearly, the presence of PTFE leads to a tremendous increase in the hydrogenation kinetics. The dehydrogenation kinetics of the loaded samples in 20% O_2/Ar is shown in Figure 1 C. It is evident that the presence of PTFE also results in a much faster dehydrogenation reaction. The data shows that the unloading kinetics decreases as the concentration of Au in the catalyst increases, irrespective of the presence of PTFE.

Hydrogenation in this case involves the dissociation of H_2 to H (Reaction 1) on the catalyst surface, the transport of H through the catalyst to the sensing layer, and H absorption by the sensing layer. The last step is governed by the thermodynamics of hydrogen absorption in Y. The improved hydrogenation kinetics of the samples in the presence of PTFE is certainly related to an increase in the H_2 adsorption/dissociation rates on the Pd_xAu_{1-x} surface. This is apparent given the fact that the sensing layer is essentially the same in each case, and especially because the effect of PTFE is limited to the catalyst surface. During dehydrogenation in O_2, H_2O is formed on the catalyst surface according to reaction steps 2–4.[32,33]

$$H_2 \rightarrow 2\,H^* \quad (1)$$

$$O_2 \rightarrow 2\,O^* \quad (2)$$

$$2\,H^* + 2\,O^* \rightarrow 2\,OH^* \quad (3)$$

$$2\,OH^* \rightarrow H_2O + O^* \quad (4)$$

Pd-catalyzed dehydrogenation of thin films in O_2 has shown to be limited by O_2 dissociation/adsorption on the surface (step 2).[31,34] Thus the observed decrease in dehydrogenation rate with increasing Au concentration is due to the fact that oxygen dissociation/adsorption is significantly higher on Pd than on Au.[15,17,35] Increasing the concentration of Au in the catalyst will lead to a decrease of the desorption kinetics because of a decrease in the number of adsorption sites available for O_2. Therefore, the response of the detector to H_2 in an O_2-rich environment is usually enhanced by alloying Pd with Au.[11] Nevertheless, we find that PTFE is able to significantly enhance the dehydrogenation rates even when the catalyst contains 20 at% Au. This suggests that the presence of PTFE promotes the dissociation/adsorption of O_2 on the catalyst, thereby enhancing the H_2O forming reaction. This explains why the hydrogenation kinetics of PTFE-capped detectors are much slower for very low concentrations of hydrogen in an oxygen-rich environments,[10] as reactions 3–4 are more favored in this case (Figure S1). No tangible difference in kinetics was observed for samples with 10–50 nm PTFE, showing that within this range the PTFE thickness does not affect the transport of H_2, O_2, and H_2O to and from the catalyst during (de)hydrogenation (Figure S2).

The kinetics of Pd-catalyzed hydrogen absorption and desorption in metal thin films have been shown to be strongly affected by the enthalpy of solution of hydrogen in the underlying metal layer.[31] To verify that the observed effect of PTFE on the kinetics is not limited to YH_x thin films, we

investigated the sensing properties of $Pd_{80}Au_{20}$ thin films with and without a PTFE top layer. This alloy on its own is an interesting H_2 sensor material with a linear relationship between the applied H_2 pressure and its reflectance and transmittance.[36] Additionally, the case of $Pd_{80}Au_{20}$ is interesting, because it can be dehydrogenated without the help of O_2 and provides therefore a suitable comparison to evaluate the unloading kinetics in the absence of O_2.[36] Figure 2 shows

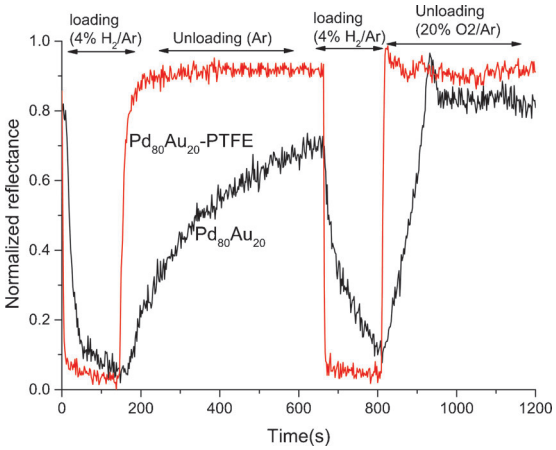

Figure 2. Effects of PTFE on the response kinetics of a 50 nm $Pd_{80}Au_{20}$ hydrogen sensor deposited on a quartz substrate.

the H_2-sensing properties of a 50 nm $Pd_{80}Au_{20}$ thin film. Clearly, the addition of a PTFE top layer leads to a visible increase in the loading kinetics and a profound increase in the unloading kinetics both in pure Ar and in 20 % O_2/Ar. Again, unloading is much faster in O_2/Ar than pure Ar, because the formation of H_2O is energetically more favorable than the recombination of atomic H to molecular H_2 that occurs in the absence of O_2. The much higher desorption kinetics of the PTFE-coated sample in Ar compared to the non-coated sample reveals that PTFE also enhances the recombination of atomic H to H_2 on the Pd–Au surface. As expected, the loading and unloading kinetics are generally faster than for the Y-Pd_xAu_{1-x} samples due to the absence of the additional step of H transport to and from the 60 nm YH_x film.[31] These results confirm that the PTFE enhanced H_2 sorption kinetics is indeed due to a change in the adsorption/dissociation of H_2 and O_2 on the Pd–Au surface. Additional experiments show that this effect is not limited to H_2 sensors as PTFE also significantly increased the kinetics of Pd-catalyzed H_2 sorption in magnesium hydride thin films used for reversible H_2 storage applications (Figure S3).

A compelling reason for this profound change in catalytic activity (adsorption/dissociation of H_2 and O_2 on Pd_xAu_{1-x}) in the presence of PTFE is a chemical or/and structural modification of the (sub)surface Pd–Au atoms by the sputtered PTFE. Such modifications will lead to a change in the binding energy of the (sub)surface atoms.[18,28] Therefore we employed X-ray photoelectron spectroscopy (XPS) to compare the electron binding energy of the sub(surface) Pd and Au (at the interface with PTFE) to that within the bulk of the Pd and Pd–Au alloy layer. Figure 3 compares the photo-

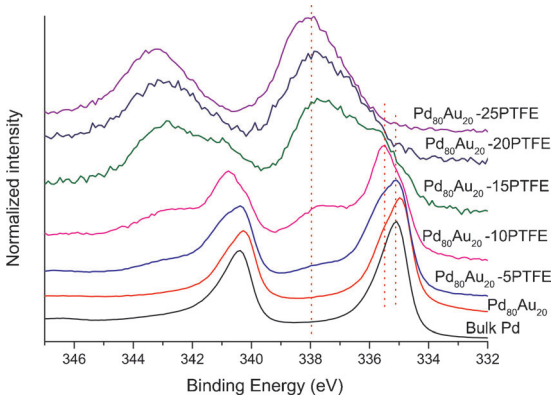

Figure 3. Comparison of the Pd ($3d_{5/2}$ and $3d_{3/2}$) XPS spectra of bulk Pd and $Pd_{80}Au_{20}$ thin films to those of $Pd_{20}Au_{20}$–PTFE samples with a 5, 10, 15, 20, and 25 nm PTFE layer.

electron signals of Pd in bulk Pd and $Pd_{80}Au_{20}$ thin films to those of Y-$Pd_{80}Au_{20}$ capped with PTFE of different thickness. Comparing the spectra of bulk Pd and $Pd_{80}Au_{20}$, we find a slight (ca. 0.2 eV) decrease in the Pd $3d_{5/2}$ and Pd $3d_{3/2}$ binding energy when Pd is alloyed with 20 at % Au. This shift is due to electron redistribution in the alloy, whereby Au loses some d electrons and gains sp electrons, whereas Pd loses sp and gains d electrons, resulting in a small net charge transfer from Pd to Au.[37,38] Interestingly, the addition of 5 or 10 nm sputtered PTFE to $Pd_{80}Au_{20}$ already results in a significant change in the Pd XPS spectra. Firstly, the $3d_{5/2}$ binding energy shifts from 335 eV in $Pd_{80}Au_2$ to 335.5 eV in $Pd_{80}Au_{20}$–10 PTFE. A similar change is also observed for Pd $3d_{3/2}$. We attribute this change to carbon implantation into Pd during the PTFE sputter deposition process leading to about 0.5 eV increase in the binding energy (when compared to bulk Pd), as reported for Pd–C_x phases.[39] Secondly, a new broad peak centered at 338.0 eV is observed for the PTFE-containing samples. This is very close to 337.7 eV reported for the rutile phase PdF_2;[40] therefore we attribute the presence of this peak to the formation of Pd–F bonds. Please note, that we do not know the exact nature of the Teflon fragments deposited. The Pd–F peak increases and becomes narrower with an increase in PTFE thickness, whereas the Pd–C peak (335.5 eV) decreases. This suggests that during PTFE sputtering some carbon is implanted into the subsurface of the catalyst layer while the Pd–F bonds are mostly formed at the catalyst surface.

Although the electron inelastic mean free path (IMFP) for bulk PTFE is approximately 3.4 nm at 1400 eV,[41] we are still able to obtain a signal from Pd capped with 25 nm sputtered PTFE. This is likely due to the huge difference between the chemical properties of bulk and sputtered PTFE (Figure 4). In addition, we believe that the sputtered PTFE is more porous than the bulk, which explains why H_2, O_2, and H_2O (formed during unloading in O_2) are easily transported to and from the catalysts even when coated with 50 nm sputtered PTFE.

Next we investigated the 1s photoelectron signals of the C and F atoms which constitutes the PTFE. Figure 4 shows that the C 1s region spectra of sputter-deposited PTFE are quite

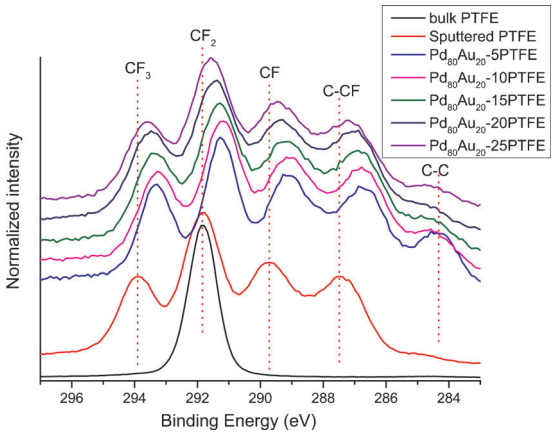

Figure 4. Comparison of the C 1s XPS spectra of bulk PTFE, 30 nm PTFE sputtered deposited on quartz (as a reference), and $Pd_{80}Au_{20}$ thin films capped with a 5, 10, 15, 20, and 25 nm sputter-deposited PTFE layer.

different from the one of the bulk. In addition to the peak at 291.8 eV due to the CF_2 bonds, three additional peaks appear in PTFE sputter-deposited on quartz. These peaks are related to the breaking and rearrangement of the C–F_2 bonds to different CF_x bonds during the deposition process.[42,43] For a 5 and 10 nm layer of PTFE on $Pd_{80}Au_{20}$, we observe a 0.9 eV decrease in the C 1s binding energy compared to CF_2. A similar decrease also occurred in the other CF_x's. This decrease in the C 1s binding energy is ascribed to the formation of Pd–CF_x bonds at the (sub)surface of the catalyst, as also seen in Figure 3 for the Pd 3d XPS. A closer look reveals that as the PTFE thickness increases, the spectra tend to shift toward the one of sputtered bulk PTFE. This is due to an increase in the ratio of the signal contributed from the upper layer of the sputtered PTFE which are not in direct contact with the Pd–Au. The corresponding region spectra for the F 1s are shown in Figure S4.

The XPS results clearly indicate that PTFE indeed modifies the chemical properties of the (sub)surface Pd–Au alloy. As no significant change is observed for Au when capped with PTFE (Figure S5), we propose that the high energy of the Teflon fragments created during sputter deposition process must have enabled the formation of different Pd–CF_x bonds at the (sub)surface of the catalyst. It appears that this chemical modification results in a more favorable interaction (adsorption/dissociation) of H_2 and O_2 on Pd and Pd–Au surfaces, leading to the improved (de)hydrogenation kinetics. As a result, the PTFE-capped H_2 detectors can be loaded and unloaded more than 40 times in H_2 and O_2, without any noticeable decrease in the kinetics (Figure S6). These findings agree well with recent results which suggest that Pd–C_x phases improve the kinetics and selectivity of Pd-based catalysts in alkyne hydrogenation and CO oxidation reactions.[39,44,45] Similarly, attaching some polymer groups on the surface of Pd nanoparticles led to improved kinetics in the Pd-catalyzed decomposition of formic acid at ambient conditions, due to surface electronic effects.[28] Our results pave the way to further improve the kinetics and tune the selectivity of Pd-based and Pd-catalyzed thin film (de)hydrogenation processes. Preliminary results show that poly(methyl methacrylate) (PMMA) and fluorinated ethylene propylene (FEP) exhibits similar effects.

In summary, the data presented here clearly show that sputtered PTFE modifies the chemical properties of (sub)surface Pd atoms in Pd–Au thin films, resulting in pronounced effects on their catalytic properties and stability in H_2 sensing and energy storage applications. This demonstrates that the combination of alloying and polymer sputtering is a promising strategy to tune the properties of thin-film-based catalysts and offers the potential for a rationale design of these catalysts with tailored properties for a variety of applications.

Received: July 5, 2014
Revised: August 8, 2014
Published online: September 22, 2014

Keywords: heterogeneous catalysis · metal hydrides · polymers · sensors · thin films

[1] F. A. Lewis, *Int. J. Hydrogen Energy* **1996**, *21*, 461 – 464.
[2] J. Tsuji, *Palladium reagents and catalysts: new perspectives for the 21st century*, Wiley, Hoboken, **2006**.
[3] T. Hübert, L. Boon-Brett, G. Black, U. Banach, *Sens. Actuators B* **2011**, *157*, 329 – 352.
[4] S. F. Silva, L. Coelho, O. Frazao, J. L. Santos, F. X. Malcata, *IEEE Sens. J.* **2012**, *12*, 93 – 102.
[5] J. Shu, B. Grandjean, A. v. Neste, S. Kaliaguine, *Can. J. Chem. Eng.* **1991**, *69*, 1036 – 1060.
[6] V. R. Choudhary, A. G. Gaikwad, S. D. Sansare, *Angew. Chem. Int. Ed.* **2001**, *40*, 1776 – 1779; *Angew. Chem.* **2001**, *113*, 1826 – 1829.
[7] A. Borgschulte, R. J. Westerwaal, J. H. Rector, H. Schreuders, B. Dam, R. Griessen, *J. Catal.* **2006**, *239*, 263 – 271.
[8] J. N. Huiberts, R. Griessen, J. H. Rector, R. J. Wijngaarden, J. P. Dekker, D. G. de Groot, N. J. Koeman, *Nature* **1996**, *380*, 231 – 234.
[9] R. Gremaud, C. P. Broedersz, D. M. Borsa, A. Borgschulte, P. Mauron, H. Schreuders, J. H. Rector, B. Dam, R. Griessen, *Adv. Mater.* **2007**, *19*, 2813 – 2817.
[10] P. Ngene, T. Radeva, M. Slaman, R. J. Westerwaal, H. Schreuders, B. Dam, *Adv. Funct. Mater.* **2014**, *24*, 2374 – 2382.
[11] M. Slaman, B. Dam, M. Pasturel, D. M. Borsa, H. Schreuders, J. H. Rector, R. Griessen, *Sens. Actuators B* **2007**, *123*, 538 – 545.
[12] J. Lee, W. Shim, E. Lee, J. S. Noh, W. Lee, *Angew. Chem. Int. Ed.* **2011**, *50*, 5301 – 5305; *Angew. Chem.* **2011**, *123*, 5413 – 5417.
[13] X. Q. Zeng, Y. L. Wang, H. Deng, M. L. Latimer, Z. L. Xiao, J. Pearson, T. Xu, H. H. Wang, U. Welp, G. W. Crabtree, W. K. Kwok, *ACS Nano* **2011**, *5*, 7443 – 7452.
[14] F. Favier, E. C. Walter, M. P. Zach, T. Benter, R. M. Penner, *Science* **2001**, *293*, 2227 – 2231.
[15] F. Abild-Pedersen, J. Greeley, F. Studt, J. Rossmeisl, T. R. Munter, P. G. Moses, E. Skúlason, T. Bligaard, J. K. Nørskov, *Phys. Rev. Lett.* **2007**, *99*, 016105.
[16] J. K. Nørskov, T. Bligaard, J. Rossmeisl, C. H. Christensen, *Nat. Chem.* **2009**, *1*, 37 – 46.
[17] F. Calle-Vallejo, J. I. Martinez, J. M. Garcia-Lastra, J. Rossmeisl, M. T. M. Koper, *Phys. Rev. Lett.* **2012**, *11*, 116103.
[18] F. Calle-Vallejo, M. T. M. Koper, A. S. Bandarenka, *Chem. Soc. Rev.* **2013**, *42*, 5210 – 5230.
[19] M. T. M. Koper, *Nanoscale* **2011**, *3*, 2054 – 2073.
[20] J. R. Kitchin, J. K. Nørskov, M. A. Barteau, J. G. Chen, *J. Chem. Phys.* **2004**, *120*, 10240 – 10246.

[21] I. E. L. Stephens, A. S. Bondarenko, F. J. Perez-Alonso, F. Calle-Vallejo, L. Bech, T. P. Johansson, A. K. Jepsen, R. Frydendal, B. P. Knudsen, J. Rossmeisl, I. Chorkendorff, *J. Am. Chem. Soc.* **2011**, *133*, 5485 – 5491.
[22] J. Knudsen, A. U. Nilekar, R. T. Vang, J. Schnadt, E. L. Kunkes, J. A. Dumesic, M. Mavrikakis, F. Besenbacher, *J. Am. Chem. Soc.* **2007**, *129*, 6485 – 6490.
[23] R. Ferrando, J. Jellinek, R. L. Johnston, *Chem. Rev.* **2008**, *108*, 845 – 910.
[24] N. Toshima, T. Yonezawa, *New J. Chem.* **1998**, *22*, 1179 – 1201.
[25] Y. Huang, X. Zhou, M. Yin, C. Liu, W. Xing, *Chem. Mater.* **2010**, *22*, 5122 – 5128.
[26] K. Tedsree, T. Li, S. Jones, C. W. A. Chan, K. M. K. Yu, P. A. J. Bagot, E. A. Marquis, G. D. W. Smith, S. C. E. Tsang, *Nat. Nanotechnol.* **2011**, *6*, 302 – 307.
[27] S. J. Tauster, S. C. Fung, R. T. K. Baker, J. A. Horsley, *Science* **1981**, *211*, 1121 – 1125.
[28] S. Jones, J. Qu, K. Tedsree, X.-Q. Gong, S. C. E. Tsang, *Angew. Chem. Int. Ed.* **2012**, *51*, 11275 – 11278; *Angew. Chem.* **2012**, *124*, 11437 – 11440.
[29] M. Slaman, B. Dam, H. Schreuders, R. Griessen, *Int. J. Hydrogen Energy* **2008**, *33*, 1084 – 1089.
[30] R. J. Westerwaal, S. Gersen, P. Ngene, H. Darmeveil, H. Schreuders, J. Middelkoop, B. Dam, *Sens. Actuators B* **2014**, *199*, 127 – 132.
[31] M. Pasturel, R. Wijngaarden, W. Lohstroh, H. Schreuders, M. Slaman, B. Dam, R. Griessen, *Chem. Mater.* **2007**, *19*, 624 – 633.
[32] C. Nyberg, C. Tengstål, *J. Chem. Phys.* **1984**, *80*, 3463 – 3468.
[33] L. G. Petersson, H. M. Dannetun, I. Lundström, *Surf. Sci.* **1985**, *161*, 77 – 100.
[34] L. Gråsjö, G. Hultquist, K. Tan, M. Seo, *Appl. Surf. Sci.* **1995**, *89*, 21 – 34.
[35] A. Staykov, T. Kamachi, T. Ishihara, K. Yoshizawa, *J. Phys. Chem. C* **2008**, *112*, 19501 – 19505.
[36] R. J. Westerwaal, J. S. A. Rooijmans, L. Leclercq, D. G. Gheorghe, T. Radeva, L. Mooij, T. Mak, L. Polak, M. Slaman, B. Dam, T. Rasing, *Int. J. Hydrogen Energy* **2013**, *38*, 4201 – 4212.
[37] Y.-S. Lee, Y. Jeon, Y.-D. Chung, K.-Y. Lim, C.-N. Whang, S.-J. Oh, *J. Korean Phys. Soc.* **2000**, *37*, 451 – 455.
[38] P. A. P. Nascente, S. G. C. de Castro, R. Landers, G. G. Kleiman, *Phys. Rev. B* **1991**, *43*, 4659 – 4666.
[39] N. Seriani, F. Mittendorfer, G. Kresse, *J. Chem. Phys.* **2010**, *132*, 024711.
[40] A. Tressaud, S. Khairoun, H. Touhara, N. Watanabe, *Z. Anorg. Allg. Chem.* **1986**, *540*, 291 – 299.
[41] P. J. Cumpson, *Surf. Interface Anal.* **2001**, *31*, 23 – 34.
[42] T. Nobuta, T. Ogawa, *J. Mater. Sci.* **2009**, *44*, 1800 – 1812.
[43] Y. Yamada, T. Kurobe, *Jpn. J. Appl. Phys.* **1993**, *32*, 5090 – 5094.
[44] O. Balmes, A. Resta, D. Wermeille, R. Felici, M. E. Messing, K. Deppert, Z. Liu, M. E. Grass, H. Bluhm, R. van Rijn, *Phys. Chem. Chem. Phys.* **2012**, *14*, 4796 – 4801.
[45] D. Teschner, J. Borsodi, A. Wootsch, Z. Révay, M. Hävecker, A. Knop-Gericke, S. D. Jackson, R. Schlögl, *Science* **2008**, *320*, 86 – 89.

